A Modular Fuel Cell, Modular DC–DC Converter Concept for High Performance and Enhanced Reliability

Leonardo Palma, *Member, IEEE*, and Prasad N. Enjeti, *Fellow, IEEE*

Abstract—Fuel cell stacks produce a dc output with a 2:1 variation in output voltage from no-load to full-load. The output voltage of each fuel cell is about 0.4 V at full-load, and several of them are connected in series to construct a stack. An example 100 V fuel cell stack consists of 250 cells in series and to produce 300 V at full-load requires 750 cells stacked in series. Since fuel cells actively convert the supplied fuel to electricity, each cell requires proper distribution of fuel, humidification, coupled with water/thermal management needs. With this added complexity, stacking more cells in series decreases the reliability of the system. For example, in the presence of bad or malperforming cell/cells in a stack, uneven heating coupled with variations in cell voltages may occur. Continuous operation under these conditions may not be possible or the overall stack output power is severely limited. In this paper, a modular fuel cell powered by a modular dc–dc converter is proposed. The proposed concept electrically divides the fuel cell stack into various sections, each powered by a dc–dc converter. The proposed modular fuel cell powered by modular dc–dc converter eliminates many of these disadvantages, resulting in a fault tolerant system. A design example is presented for a 150-W, three-section fuel cell stack and dc–dc converter topology. Experimental results obtained on a 150-W, three-section proton exchange membrane (PEM) fuel cell stack powered by a modular dc–dc converter are discussed.

Index Terms—DC–DC converters, fuel cells, power conditioning, renewable power.

I. INTRODUCTION

FUEL CELLS are electrochemical devices that process H_2 and oxygen to generate electric power, having water vapor as their only by-product. The voltage resulting from the reaction of the fuel and oxygen varies with the load, and ranges from 0.8 V at no-load to about 0.4 V for full-load. Due to their low output voltage, it becomes necessary to stack many cells in series to realize a practical system.

For low-power applications, the number of cells that needs to be connected in series is small, but as power increases, the number of cells that are required in the stack increases rapidly [1], [2]. An example 100 V fuel cell stack consists of 250 cells in series and to produce 300 V at full-load requires 750 cells stacked in series. A conventional fuel cell system (Fig. 1) consists of a stack of cells and a dc–dc converter to

L. Palma is with the Universidad de Concepción, Concepción 4030000, Chile (e-mail: palma@ieee.org).

P. N. Enjeti is with the Power Electronics and Fuel Cell Power Conversion Laboratory, Department of Electrical and Computer Engineering, Texas A&M University, College Station, TX 77840 USA (e-mail: enjeti@tamu.edu).
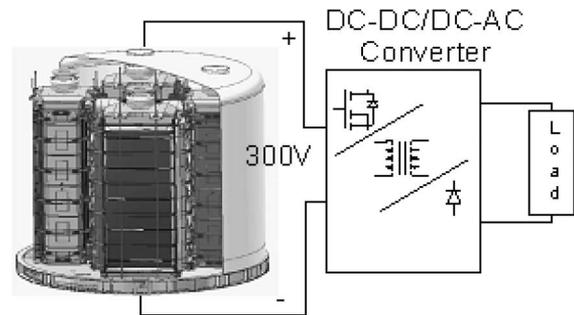
Fig. 1. Utility scale fuel cell stack and dc–dc/dc–ac converter.
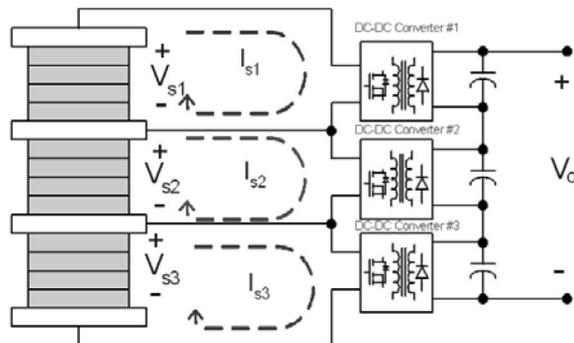

Fig. 2. Proposed modular fuel cell and modular dc–dc converter concept.

step-up its terminal voltage and compensate for its no-load to full-load variation [3]–[5]. Since this fuel cell structure is equivalent to connecting several voltage sources in series, each with its own internal impedance [6], [7], the output power of the stack is limited by the state of the weakest cell. The state of a cell can be inferred from the voltage across its terminals, which is affected by parameters such as fuel and air pressure, and membrane humidity. Furthermore, if a stack contains malfunctioning or defective cells, the whole system has to be taken out of service until major repairs are done.

In order to circumvent these problems, a modular fuel cell powered by a modular dc–dc converter (Fig. 2) is proposed in this paper. The proposed modular concept electrically divides the fuel cell stack into various sections, each powered by a dc–dc converter. This modular fuel cell powered by modular dc–dc converter eliminates many of the disadvantages, resulting in a fault tolerant system. A design example is presented for a 150-W, three-section fuel cell stack and dc–dc converter topology. Experimental results obtained on a 150-W, three-section

proton exchange membrane (PEM) fuel cell stack powered by a modular dc–dc converter are discussed. The proposed system has the following advantages.

1) The power generated by different sections in the modular fuel cell stack can be independently controlled by each dc–dc converter.

2) Extra heating in underperforming sections of the stack, due to their larger internal impedance, can be reduced by limiting their load current, thus reducing the internal losses in the fuel cell.

3) If a section of the stack is faulty, the dc–dc converter controlling the faulty section can be disenabled and/or bypassed, while the rest of the system can continue operation at reduced power.

4) If the proposed modular stack is employed in automotive systems, under faults, the driver can steer the vehicle to a safe location at reduced power, since faulty stack sections can be shut down.

Different modular topologies have been explored in the past for application on photovoltaic (PV) systems aimed mainly to reduce the need of having long strings of panels [8]. However, for the case of fuel cell systems, due to their physical construction, long stacks of cells are not avoidable. Instead, the main concern is overheating and loss of output power due to the presence of bad cells in the stack. Thus, a different converter structure, control scheme, and modified stack structure become necessary.

II. MODULAR FUEL CELL STACK

Fuel cell stacks are constructed by stacking several individual cells, which is equivalent to connecting many voltage sources in series, each with its own internal impedance. The fuel and oxygen input lines to each cell in the stack are connected in parallel in order to ensure that the pressure on the anode and cathode of every cell is kept at a similar level. This is done by means of manifolds that connect the fuel and oxygen lines to the actual cells in the stack. The voltage produced by each cell in the stack, as well as its internal impedance, is a function of fuel pressure, membrane humidity, and state of the catalyst. The fuel pressure on each cell is, in theory, constant due to the input manifold, but in reality, it may drop due to water condensation or other obstructions. Cells receiving a lower pressure will produce a reduced voltage. The membrane humidity may vary from cell to cell depending on the heat distribution within the fuel cell. Cells with a drier membrane will produce less voltage than cells with a more moisturized membrane, and this will produce a voltage closer to its nominal. All these reasons contribute to an uneven voltage distribution through the fuel cell stack.

As an example, Fig. 3 shows the V–I characteristic measured from different cells in a 24-cell 12-V/150-W H_2–air PEM fuel cell stack with an active area of $50\,cm^2$. The characteristics were obtained at room temperature (20°C) with a fuel pressure of $2\,lbf/in^2$; the maximum cell temperature was measured to be $62\,°C$.

It is clear from Fig. 3 that the voltage produced by each cell in the stack differs from adjacent cells. Further, a set of cells is shown to produce less voltage when compared to a
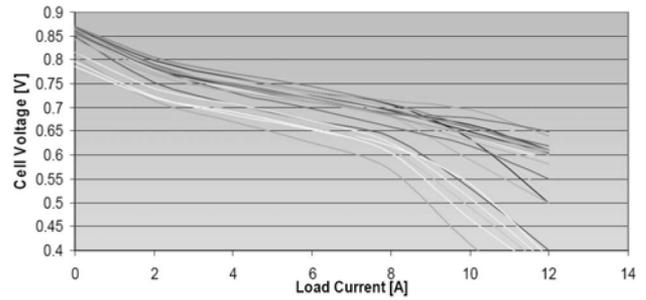
Fig. 3.   Individual cell V–I curves for the 12-V, 150-W, 24-cell fuel cell stack.
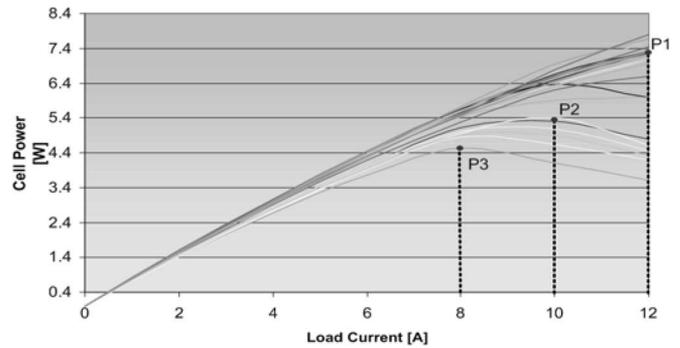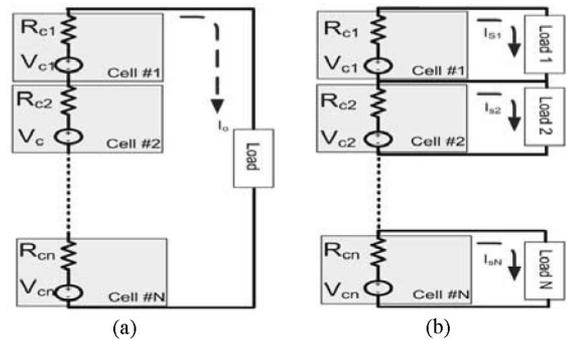
Fig. 4.   Individual cell P–I.

Fig. 5.   Modular fuel cell simplified equivalent circuit.

healthier group. Fig. 4 shows the power (in watts) generated by each individual cell in this test stack. Comparing the maximum power points P1, P2, and P3 in Fig. 4, it becomes evident that underperforming cells in the fuel cell can produce less power than the cells that are in good operating condition.

Although, as shown in Fig. 3, fuel cells exhibit a nonlinear behavior in their voltage–current characteristic, it is possible to use a linearized model to predict their behavior. In steady state, the simplest electrical model that can be constructed consists of a Thevenin voltage source (V_c) in series with a resistor (R_c) [Fig. 5(a)] whose values are functions of fuel pressure, humidity, and catalyst state, as discussed before.

From this equivalent circuit model, the power that a single cell in the stack can supply can be calculated by

$$P_o = V_C I_o - R_C I_o^2. \tag{1}$$

TABLE I
EQUIVALENT CIRCUIT PARAMETERS

	V_c	R_c
Cell 1	1.00Va	1.0Ra
Cell 2	0.95Va	1.3Ra
Cell 3	0.90Va	1.4Ra

Additionally, from circuit theory, the maximum power that can be extracted from such an electric circuit is given by

$$P_{\max} = \frac{V_C^2}{4R_c}. \tag{2}$$

From (1) and (2), it is apparent that increasing the load of the fuel cell beyond the maximum power point given by (2) results in increased losses and reduced output power, as can be observed from Fig. 4. Therefore, the load current should be limited to avoid going beyond the maximum power point to a value given by

$$I_{o\,\max} = \frac{V_C}{2R_C}. \tag{3}$$

Further, since in a conventional system all the cells in the stack are connected in series, the load current in every cell has to be limited to the maximum current that the weakest cell in the system can supply, which is around 8 A in the case shown in Figs. 3 and 4. Considering this fact, the maximum output power of the stack can be calculated by

$$P_{\max} = \sum_{n=1}^{N} V_{Cn} I_{o\,\max} - R_{Cn} I_{o\,\max}^2. \tag{4}$$

If the load current exceeds the limit given by (3) for a long period of time, the stack overheats due to the additional internal losses in the malperforming cells, and operation of the fuel cell has to be discontinued. However, from Fig. 4, it is clear that healthier cells, which have a smaller internal resistance and larger open circuit voltage, can supply higher load currents (10 or 12 A).

From this analysis, it appears that to avoid limiting the current in healthy cells due to the presence of bad cells in the system, a modular approach is more suitable. This modular system is shown in Fig. 5(b), where additional terminals on each cell allow loading cells independently, and therefore, healthier cells can generate more power than in the conventional series-connected approach. For this modular case, the maximum power that can be generated in the stack is given by the sum of the maximum powers of all cells, and can be calculated by

$$P_{\max} = \sum_{n=1}^{N} \frac{V_{Cn}^2}{4R_{Cn}}. \tag{5}$$

To compare both approaches, traditional and modular, the maximum power that can be produced by each is evaluated. For this, let us consider a stack constructed with three cells and with the equivalent circuit parameters as shown in Table I, where V_a and R_a are the base voltage and resistance of the system.

Using the parameters of Table I and (3), we can find that in the case of the conventional approach, the load current should be limited to $0.32\,V_a/R_a$; this is due to the internal impedance
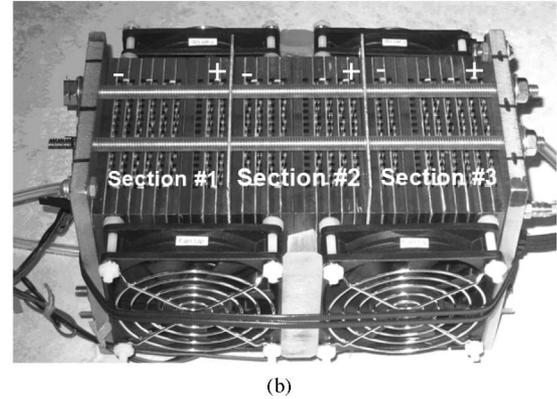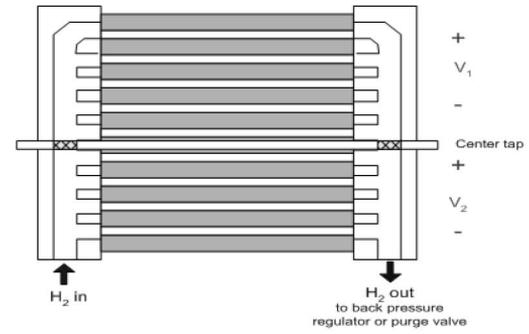

(a)

(b)

Fig. 6.   (a) Schematic drawing of the modular fuel cell stack. (b) Prototype of the 12-V, 150-W, 24-cell modular fuel cell stack.

of cell 3, which is the weakest cell in this stack. Thus, according to (4), the maximum power that can be produced in this case is $0.534\,V_a^2/R_a$. Now, for the modular approach where each cell is loaded independently [Fig. 5(b)] using (5), the maximum power that the system can generate is $0.568\,V_a^2/R_a$. In other words, the same stack can produce 6.4% more power if the cells are loaded independently.

From these results, it is shown that to optimize the operation of the stack, one should be able to control the current flowing through each individual cell in the stack [Fig. 5(b)]. But such an approach proves to be impractical as well as uneconomical. A more convenient approach is to divide the stack in sections of five to ten cells, as shown in Fig. 2, which is done by installing additional electric terminals in the stack (Fig. 6). Having access to these additional terminals allows loading each section differently, which, in turn, allows maximizing the power generated by the stack.

This has the obvious advantage of increasing the overall reliability of the system. Fig. 7 shows the V–I characteristic of each of the three sections in the prototype fuel cell stack measured at room temperature with a fuel pressure of $2\,\text{lbf/in}^2$. It can be observed that the performance of each of the sections is quite different. The nominal current of the stack (12 A) can only be drawn from sections 1 and 3. On the other hand, section 2 can only supply a maximum current of 9 A before its voltage collapses.

Fig. 8 shows the power produced by each section in the fuel cell stack as function of the load current. If a traditional approach is used, to avoid overheating, the current in the stack should be limited to a value given by its weakest section (section 2, 9 A),
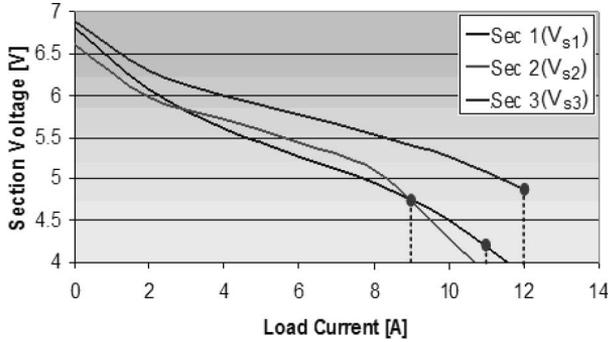
Fig. 7. $V-I$ characteristics of the proposed modular fuel cell stack with three sections.
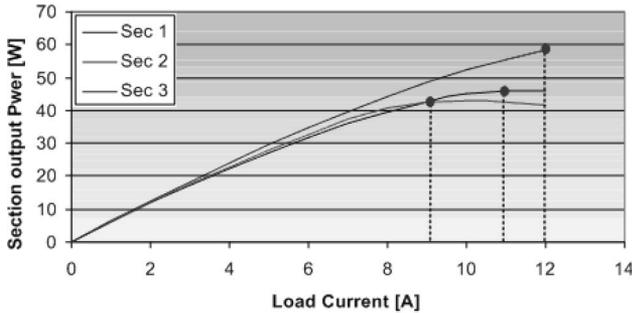

Fig. 8. Output power produced by each section of the modular fuel cell stack.

TABLE II
CONVENTIONAL AND MODULAR APPROACH COMPARISON

	Conventional	Modular
Section 1	42 W	42 W
Section 2	43 W	47 W
Section 3	49 W	58 W
Total power	134 W	147 W

but due to the modular construction of the system, the other sections can be operated at different load currents to optimize their operation. Table II shows a comparison of the power that this prototype stack can produce if operated in a traditional or modular fashion. These results are obtained from Fig. 8, and the results for the traditional approach are obtained by multiplying the section voltages by the maximum current that the weakest section can produce (9 A). On the other hand, the power for the modular approach is calculated from the maximum power point for each of the sections in Fig. 8. It can be seen from Table II that by loading each section of the proposed modular stack differently, the fuel cell can produce 10% more power than using a conventional stack. Moreover, this result shows that despite having underperforming cells in the system, the power generated is close to the stack nominal.

III. PROPOSED MODULAR DC–DC CONVERTER

To take advantage of the modular fuel cell stack, an appropriate dc–dc converter and control scheme are required. The converter should have as many independently controllable inputs as there are sections in the stack. In addition, since the positive terminal of one section in the stack also serves as the
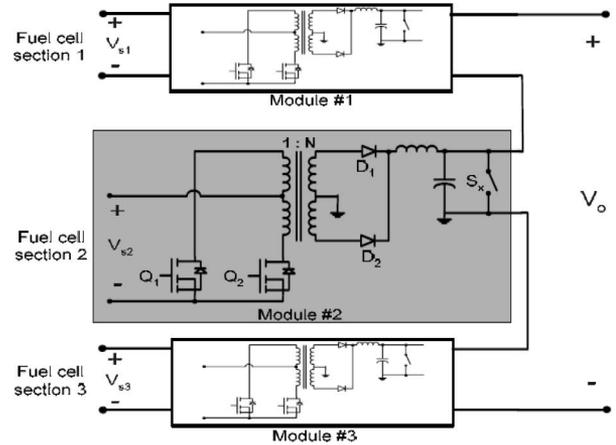

Fig. 9. Proposed modular dc–dc converter.

negative terminal for the next section, the converter should provide isolation between its input and output to avoid circulating currents. A converter meeting these specifications can be constructed by using an arrangement of isolated dc–dc converter modules, where the inputs of each module are connected across each of the sections of the stack and their outputs are connected in series in order to add the output voltages of the different modules, thus obtaining a higher output voltage. Such a modular dc–dc converter is shown in Fig. 9, where the converter is composed of three push–pull modules.

As discussed earlier, another advantage of constructing a fuel cell stack with several sections is that faulty portions of the stack can be bypassed, while the rest of the stack can continue operation. To implement this function, each of the modules used to construct the dc–dc converter should be able to stop extracting power from the section they are connected to and set its output impedance to zero. This function can be accomplished by removing the gating signals to the transistors. In addition, it is necessary to add a switch (S_x) at the output of each module to short-circuit the output capacitor of the module and bypass it.

In order to optimize the power extraction from each of the sections in the fuel cell, an appropriate control scheme needs to be devised. From Figs. 7 and 8, it can be observed that the voltage across the terminals of each section in the stack is a good indication of how much power it can generate; thus, this information can be used to better distribute the power extracted from each section.

A section producing a higher voltage can generate more power than a section that produces a lower voltage. Therefore, by controlling the load current on each section in the stack as a function of the voltage, they produce results in healthier sections supplying more power than underperforming sections. This, in turn, reduces internal losses and improves the overall efficiency of the system. Since the outputs of the modules are connected in series, their output currents i_o are identical.

Now, if the modules are constructed by push–pull converters, the input current of every module is given by (6), where D_n is the duty cycle of the nth module and N_1 and N_2 are the transformer primary and secondary turns
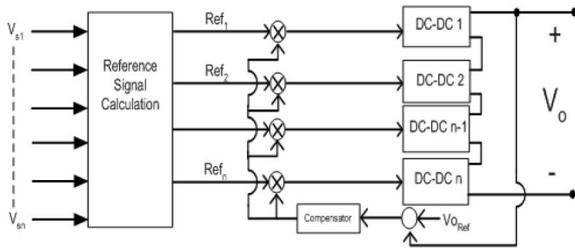
$$i_{\text{in},n} = \frac{N_2}{N_1} D_n i_o. \tag{6}$$

Fig. 10. Proposed control scheme.

Fig. 11. Modular fuel cell section voltages during a load transient.

Thus, the input current of each module can be controlled by setting an appropriate duty cycle. The duty cycle for each module is calculated as shown in Fig. 10. In this block diagram, the output voltage of the converter is maintained constant to the value set by $V_{o,\text{ref}}$. The output of the main voltage loop compensator is then used to calculate the required duty cycle for each dc–dc converter by multiplying it with the corresponding reference signal for each module. These reference signals are calculated by taking into account the voltage produced by each of the sections in the stack and the number of modules that compose the dc–dc converter. Each of the reference signals is calculated by the weighting function shown as

$$\text{Ref}_n = \frac{V_{Sn}}{\sum_{i=1}^{\text{NAC}} V_{Si}} \qquad (7)$$

where V_{Sn} is the voltage produced by the "nth" section in the fuel cell stack, V_{Si} is the voltage produced by the "ith" section in the stack, and NAC is the total number of active sections in the stack. Thus, the reference signal for the "nth" module is given by the ratio between the voltage produced by the "nth" section in stack and the total voltage produced by the stack. The number of active sections is defined by all the sections that produce a voltage above a minimum value. Now, if one of the sections produces a voltage below this threshold level, then that section can be considered faulty. Thus, it cannot produce power and needs to be discarded. In this case, the controller reduces NAC by 1 and sets the reference signal to the respective module to zero. Additionally, this has the effect of increasing the reference signals of the remaining modules to compensate for the loss of one stack section.

The implementation of this control scheme can be carried out by combining digital and analog controllers. The calculation of the reference signals for each of the modules is done digitally by means of a DSP. The reference signals are then feed to analog controllers located on each of the dc–dc modules.

IV. EXPERIMENTAL RESULTS

To verify the operation of the proposed fuel cell stack and converter, a laboratory prototype was built. The test system is composed of a 12-V/150-W H_2–air PEM modular fuel cell stack consisting of three sections of eight cells, each with an active area of $50\,\text{cm}^2$, and a modular dc–dc converter composed of three push–pull modules. The dc–dc converter is designed to supply a 22-V load; thus, if all the sections in the fuel cell produce the same voltage across their terminals, each module
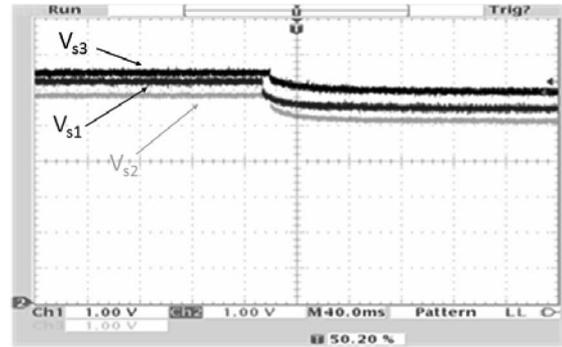
needs to provide one-third of the total output voltage V_o and output power. However, since the dc–dc converter has to be designed for continue operation under the condition of having faulty sections, each module is designed in order to provide the total output voltage V_o of the converter and one-third of its output power, i.e., 22 V and 50 W. The dc–dc converter and modules are connected as shown in the schematic in Fig. 9. This prototype system was tested at room temperature and with an H_2 supply at a pressure of $2\,\text{lbf/in}^2$.

As a first test, a load change is applied at the output terminals of the converter to verify that the controller adjusts the loading of each section according to their relative health. Fig. 11 shows the voltage across each of the sections in the prototype stack when the output load of the system increases from 40% to 90%. During this test, the voltage at the output terminals of the converter was maintained constant at 22 V. In this figure, Ch. 1 shows the voltage in section 3 (V_{s3}), Ch. 2 the voltage in section 1 (V_{s1}), and Ch. 3 the voltage in section 2 (V_{s2}). As can be seen from Fig. 11, initially, the voltages of the three sections were 6.4, 5.6, and 6.2 V, respectively. After the load increases, the controller adjusts the module reference signals in order to maintain the output voltage of the converter constant. And thus, the three section voltages drop due to the increase in the output load to 6, 5.5, and 5 V.

Fig. 12 shows the current drawn from each section in the stack before and after the load change. As can be observed from these results before the load change, the voltage supplied by section 3 was the highest in the stack; consequently, the current and power supplied by it are the highest. On the other hand, the voltage produced by section 2 in the prototype stack is the lowest, and therefore, the current drawn from it is less than the other two sections.

After the transient, the voltage across each section drops due to the increase in output load, and the currents drawn from the three sections increase to maintain the output voltage of the system constant; however, their magnitudes are different. As can be seen from Figs. 11 and 12, the section producing the highest voltage carries a larger share of the output power and the weakest section produces a smaller portion of the load.

The other functionality offered by the proposed converter is the ability to discard a section of the fuel cell if the controller detects that the voltage across its terminals drops below a certain
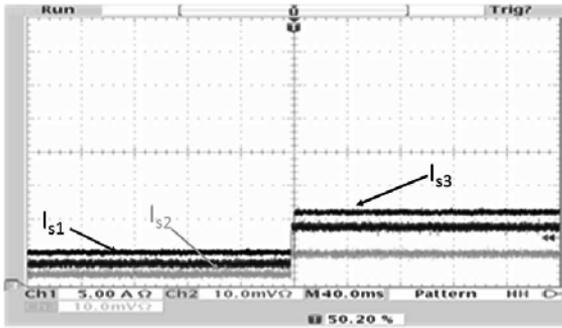
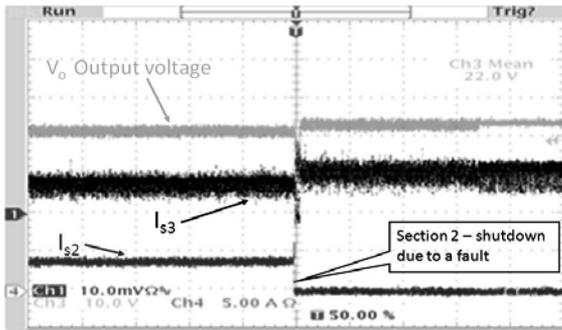Fig. 12. Modular fuel cell section currents during a load transient.

(a)

Fig. 13. Operation of the modular fuel cell modular dc–dc converter under a fault. Note that in section 2, current is reduced to zero, while the output voltage continues to be regulated.

(b)

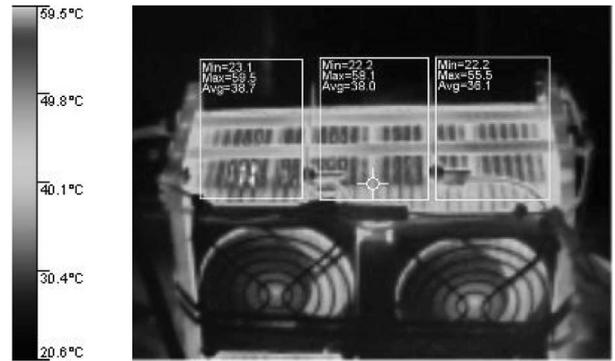Fig. 14. Thermal comparison of conventional and modular fuel cell.

threshold level. The prototype fuel cell is rated for 12 V at full-load, and the nominal voltage of each of the sections at full-load is 4 V. Therefore, if a section is faulty, its terminal voltage will fall below this value. For this reason, the threshold level in the controller was set to 3.8 V. Fig. 13 shows the behavior of the system when a faulty section is detected, where Ch. 1 corresponds to the current drawn from section 3 (I_{s3}), Ch. 3 the output voltage of the dc–dc converter (V_o), and Ch. 4 the current drawn from section 2 (I_{s2}).

In this case, section 2 in the stack is faulty, and it has to be discarded to avoid stack shutdown due to overheating. As can be seen in Fig. 13, once the fault condition is detected, the current drawn from the faulty section (section 2, Ch. 4) falls to zero. In order to maintain the output voltage of the system constant, the currents drawn from the remaining sections in the stack (I_{s1} and I_{s3}) have to increase. This can be observed from Fig. 13, where the current supplied by section 3 (I_{s3}) increases from 5 to 7 A after section 2 is discarded. The increase in the magnitude of the currents drawn from the remaining sections is regulated in terms of their relative health as determined by the converter control. As can be seen from these results, the system can continue operation despite having a faulty section; thus, the modular approach exhibits higher reliability than the traditional approach.

To further verify the effectiveness of the proposed approach, thermal images of the fuel cell stack operating in both single stack and modular stack modes were taken. Fig. 14(a) shows a thermal image of the prototype stack operating in conventional mode. Load current in this case is 7.25 A, and the voltage of the

stack was measured to be 12 V, which is the nominal voltage of the fuel cell for full-load. The power generated by the stack operating under this condition was measured to be 87 W. It can be observed that the temperature distribution is quite uneven due to the presence of bad cells in section 2, while sections 1 and 3 show a lower temperature indicating that they are underused.

The result of reconfiguring the stack for modular operation and the use of the proposed dc–dc converter is shown in Fig. 14(b). In this case, the voltage across each of the sections was regulated by the dc–dc converter modules to 4 V, i.e., the nominal voltage for each section. The currents drawn from sections 1–3 in the stack were measured to be 10, 6, and 9 A, respectively. Thus, the power generated by the fuel cell in this case is 102 W. As can be seen from Fig. 14(b), the temperature distribution within the stack in this case is even, indicating full utilization of the three sections. Moreover, due to the use of the modular approach, the fuel cell generates 15% more power than in the conventional case [Fig. 14(a)].

V. CONCLUSION

In this paper, a modular fuel cell stack and dc–dc converter concept has been presented. It has been shown that the standard fuel cell stack can be reconfigured into several sections with smaller cell count, each supplying an isolated power module in the dc–dc converter, resulting in a high-performance system. The proposed system has been shown to be fault tolerant and can continue to operate at a reduced power level under fuel cell

or power module faults. Experimental results on a 12-V/150-W system demonstrate that under normal operation, the proposed system is capable of producing 10% additional power when compared to the traditional approach. In addition, experimental results also confirm the operation of the system under stack failure.

REFERENCES

[1] L. Palma and P. Enjeti, "A modular fuel cell, modular DC–DC converter concept," Texas A& M University, College Station, TAMUS 2431 Invention disclosure, Sep. 2006.

[2] M. Ellis, M. Spakovsky, and D. Nelson, "Fuel cell systems: Efficient, flexible energy conversion for the 21st century," *Proc. IEEE*, vol. 89, no. 12, pp. 1808–1818, Dec. 2001.

[3] R. Gopinath, K. Sangsun, H. Jae-Hong, P. N. Enjeti, M. B. Yeary, and J. W. Howze, "Development of a low cost fuel cell inverter system with DSP control," *IEEE Trans. Power Electron.*, vol. 19, no. 5, pp. 1256–1262, Sep. 2004.

[4] R.-J. Wai and R.-Y. Duan, "High-efficiency power conversion for low power fuel cell generation system," *IEEE Trans. Power Electron.*, vol. 20, no. 4, pp. 847–856, Jul. 2005.

[5] B. Bouneb, D. M. Grant, A. Cruden, and J. R. McDonald, "Grid connected inverter suitable for economic residential fuel cell operation," in *Proc. Eur. Conf. Power Electron. Appl.*, Sep. 11-14, 2005, p. 10.

[6] R. Amphlett, R. Mann, B. Peppley, P. Roberge, and A. Rodigues, "A practical PEM fuel cell model for simulation vehicle power sources," in *Proc. 10th Annu. Battery Conf. Appl. Adv. 1995*, Jan. 10–13, pp. 221–226.

[7] W. Friede, S. Rael, and B. Davat, "Mathematical model and characterization of the transient behavior of a PEM fuel cell," *IEEE Trans. Power Electron.*, vol. 19, no. 5, pp. 1234–1241, Sep. 2004.

[8] R. M. Button, "An advanced photovoltaic array regulator module," in *Proc. 31st Intersoc. Energy Convers. Eng. Conf. (IECEC 1996)*, Aug. 11–16, vol. 1, pp. 519–524.

[9] R. Ayyanar, R. Giri, and N. Mohan, "Active input-voltage and load-current sharing in input-series and output-parallel connected modular DC–DC converters using dynamic input-voltage reference scheme," *IEEE Trans. Power Electron.*, vol. 19, no. 6, pp. 1462–1473, Nov. 2004.

[10] E. Cengelci, P. Enjeti, and J. W. Gray, "A new modular motor-modular inverter concept for medium-voltage adjustable-speed-drive systems," *IEEE Trans. Ind. Appl.*, vol. 36, no. 3, pp. 786–796, May/Jun. 2000.

[11] L. M. Tolbert and F. Z. Peng, "Multilevel converters as a utility interface for renewable energy systems," in *Proc. IEEE Power Eng. Soc. Summer Meeting 2000*, Jul. 16–20, vol. 2, pp. 1271–1274.

[12] R. Erickson and D. Maksimovic, *Fundamentals of Power Electronics*. Norwell, MA: Kluwer, 2001.

[13] C. Liu and J.-S. Lai, "Low frequency current ripple reduction technique with active control in a fuel cell power system with inverter load," *IEEE Trans. Power Electron.*, vol. 22, no. 4, pp. 1429–1436, Jul. 2007.

[14] B. Ozpineci, L. M. Tolbert, G.-J. Su, and Z. Du, "Optimum fuel cell utilization with multilevel DC–DC converters," in *Proc. 19th Annu. IEEE Appl. Power Electron. Conf. Expo. (APEC 2004)*, vol. 3, pp. 1572–1576.

[15] F. Richardeau, P. Baudesson, and T. A. Meynard, "Failures-tolerance and remedial strategies of a PWM multicell inverter," *IEEE Trans. Power Electron.*, vol. 17, no. 6, pp. 905–912, Nov. 2002.

[16] C. Turpin, F. Forest, F. Richardeau, T. A. Meynard, and A. Lacarnoy, "Switching faults and safe control of an ARCP multicell flying capacitor inverter," *IEEE Trans. Power Electron.*, vol. 18, no. 5, pp. 1158–1167, Sep. 2003.

[17] C. A. Martins, X. Roboam, T. A. Meynard, and A. S. Carvalho, "Switching frequency imposition and ripple reduction in DTC drives by using a multilevel converter," *IEEE Trans. Power Electron.*, vol. 17, no. 2, pp. 286–297, Mar. 2002.

[18] G. Fontes, C. Turpin, S. Astier, and T. A. Meynar, "Interactions between fuel cells and power converters: Influence of current harmonics on a fuel cell stack," *IEEE Trans. Power Electron.*, vol. 22, no. 2, pp. 670–678, Mar. 2007.

[19] A. Emadi, S. S. Williamson, and A. Khaligh, "Power electronics intensive solutions for advanced electric, hybrid electric, and fuel cell vehicular power systems," *IEEE Trans. Power Electron.*, vol. 21, no. 3, pp. 567–577, May 2006.

[20] R. Sharma and H. Gao, "Low cost high efficiency DC–DC converter for fuel cell powered auxiliary power unit of a heavy vehicle," *IEEE Trans. Power Electron.*, vol. 21, no. 3, pp. 587–591, May 2006.

[21] H.-J. Chiu and L.-W. Li, "A bidirectional DC–DC converter for fuel cell electric vehicle driving system," *IEEE Trans. Power Electron.*, vol. 21, no. 4, pp. 950–958, Jul. 2006.

[22] M. Marchesoni and C. Vacca, "New DC–DC converter for energy storage system interfacing in fuel cell hybrid electric vehicles," *IEEE Trans. Power Electron.*, vol. 22, no. 1, pp. 301–308, Jan. 2007.

[23] J. L. Duarte, M. Hendrix, and M. G. Simoes, "Three-port bidirectional converter for hybrid fuel cell systems," *IEEE Trans. Power Electron.*, vol. 22, no. 2, pp. 480–487, Mar. 2007.

[24] X. Kong and A. M. Khambadkone, "Analysis and implementation of a high efficiency, interleaved current-fed full bridge converter for fuel cell system," *IEEE Trans. Power Electron.*, vol. 22, no. 2, pp. 543–550, Mar. 2007.

[25] G. Fontes, C. Turpin, S. Astier, and T. A. Meynard, "Interactions between fuel cells and power converters: Influence of current harmonics on a fuel cell stack," *IEEE Trans. Power Electron.*, vol. 22, no. 2, pp. 670–678, Mar. 2007.

[26] N. D. Benavides and P. L. Chapman, "Mass-optimal design methodology for DC–DC converters in low-power portable fuel cell applications," *IEEE Trans. Power Electron.*, vol. 23, no. 3, pp. 1545–1555, May 2008.

Leonardo Palma (S'02–M'07) received the B.S. degree in electrical engineering from the Universidad de Concepción, Concepción, Chile, in 1999, and the M.S. and Ph.D. degrees from Texas A&M University, College Station, in 2003 and 2006, respectively.

He is currently an Assistant Professor at the Universidad de Concepción. His current research interests include theory and applications in the areas of distributed energy systems, green power, power supplies, motor drives, and modern energy storage devices.

Prasad N. Enjeti (M'85–SM'88–F'00) received the B.E. degree in electrical engineering from Osmania University, Hyderabad, India, in 1980, the M.Tech. degree in electrical engineering from the Indian Institute of Technology Kanpur, Kanpur, India, in 1982, and the Ph.D. degree in electrical engineering from Concordia University, Montreal, QC, Canada, in 1988.

In 1988, he joined the Department of Electrical Engineering, Texas A&M University, College Station, as an Assistant Professor, where he was promoted to an Associate Professor in 1994, became a Full Professor in 1998, and is the Lead Developer of the Power Electronics/Power Quality and Fuel Cell Power Conditioning Laboratories. He is actively involved in many projects with industries while engaged in teaching, research, and consulting in the area of power electronics, motor drives, power quality, and clean power utility interface issues. He is the holder of four U.S. patents and has licensed two new technologies to the industry so far. His current research interests include advanced converters for power supplies and motor drives, power quality issues, active power filter development, utility interface issues, advancing switching power supply designs and solutions to complex power management issues in the context of analog and mixed-signal applications, exploring alternative designs to meet the demands of high slew rate load currents at low output voltages, power conditioning systems for fuel cells, wind, and solar energy systems, and design of high-temperature power conversion systems with wideband gap semiconductor devices.

Dr. Enjeti is the recipient of the select title "Class of 2001 Texas A&M University Faculty Fellow" Award for demonstrated achievement of excellence in research, scholarship, and leadership in the field. He was the recipient of the IEEE–Industry Applications Society (IAS) Second and Third Best Paper Awards in 1993, 1998, 1999, 2001, and 1996, respectively, the Second Best IEEE-IA Transactions Paper published in midyear 1994 to midyear 1995, and the IEEE–IAS Magazine Prize Article Award in 1996. In 2000, he was elected as a Fellow by the IEEE Fellows Committee for "Contributions to solutions of utility interface problems in power electronic systems and harmonic mitigation." He directed a team of students to design and build a low-cost fuel cell inverter for residential applications, which won the 2001 Future Energy Challenge Award Grand Prize from the Department of Energy. He is a Registered Professional Engineer in Texas.